



Effect of Different Arrangements of CFRP Wraps on the Axial Stress–Strain Behaviour of Confined Concrete Cylinders: Experimental Study and Numerical Modelling

Arash Totonchi¹ · Ahmadreza Ansaripour² · Sina Shivaie³ 

Received: 31 August 2018 / Accepted: 15 July 2019 / Published online: 22 July 2019
© Shiraz University 2019

Abstract

Concrete columns externally confined with carbon fibre-reinforced polymer (CFRP) composites have demonstrated considerable improvements in the axial stress–strain behaviour. In some cases, the CFRP partial or discontinuous wrapping strengthening technique tends to be at an advantage over the full wrapping strengthening method. Discontinuous or partial confinement of circular concrete columns employing CFRP laminates strips or wraps can be an efficient method of structural rehabilitation and strengthening. A series of axial compression tests on standard cylindrical concrete specimens confined with different arrangements of strips of CFRP laminates were used to verify the finite element (FE) model. A three-dimensional nonlinear FE approach for concrete subjected to monotonic loading was employed. Comparison between the axial stress–strain behaviour of partially or discontinuously confined concrete cylinders with the same ratio of bonding area of CFRP laminates and that of fully CFRP-wrapped as well as unwrapped cylinders has been drawn. It was concluded that different arrangements of discontinuous CFRP laminates strips did not have any noticeable effect on the axial stress–strain behaviour of concrete specimens, while the change in the position and width of partial CFRP wraps significantly affected the axial stress–strain behaviour of concrete specimens. Finally, the failure pattern of discontinuously CFRP-wrapped concrete cylinders has been examined.

Keywords CFRP arrangement · Experimental · Finite element · Concrete cylinder · Discontinuously wrapped · Partially wrapped

1 Introduction

Rarely have the vast majority of concrete structures met new regulations due to human factors such as faulty construction practices, computational errors, use of sub-standard quality

of construction material, and an increase in the load capacity of structures for carrying additional loads. Furthermore, extreme weather conditions play a major part in ageing and structural deterioration. Above all, massive earthquakes can cause severe damage to concrete structures, being responsible for insufficient lateral strength and a rapid reduction in structural resistance. In many cases, restoring and renovating structural elements should be taken into consideration in order to minimize potential damage.

Reinforced concrete columns, the load-bearing elements of every structure, bearing pure axial load or bending moment along with axial load simultaneously, are one of the most critical parts of buildings and bridges (Zaki 2011). These vertical elements should be designed in such a way that they exhibit ductile behaviour. The confinement of concrete using fibre-reinforced polymer (FRP) composites has been considered as one of the most tried-and-tested methods for providing ductility, as well as strengthening and increasing the bearing capacity of concrete columns amongst civil

✉ Sina Shivaie
sina.shivaie@gmail.com

Arash Totonchi
Totonchi@miau.ac.ir

Ahadreza Ansaripour
ahmadre67@gmail.com

¹ Department of Civil Engineering, Islamic Azad University, Marvdasht Branch, Marvdasht, Iran
² Department of Civil Engineering, Apadana Institute of Higher Education, Shiraz, Iran
³ Department of Civil and Environmental Engineering, Shiraz University, Shiraz, Iran

engineers. There are several advantages to utilizing FRP composites as confining materials. Firstly, such composite materials restrict the radial expansion of columns; subsequently, the detachment of concrete crust is postponed, preventing the buckling of longitudinal reinforcement of columns and finally avoid column destruction (Saadatmand 2003).

Ongoing developments in science in recent years, especially in civil engineering, have led to researchers taking full advantage of innovative methods and synthetic materials. Amongst new materials, carbon fibre-reinforced polymer (CFRP) composites have received wider currency. CFRP composites have been attached with more significance owing to their high tensile strength, high strength-to-weight ratio, speed and ease of installation, and corrosion resistance (Das and Nizam 2014). For the first time in the mid-eighties, CFRP composites were introduced to confine concrete columns against strong earthquakes (Busel and White 2003). Then, in 1991, CFRP composites were employed to strengthen reinforced concrete bridges. Both earthquakes which struck Southern California in 1990 and Kobe (Japan) in 1995 led to further investigation into using CFRP composites to strengthen concrete structures in earthquake-prone areas. Saafi et al. (1999) used a number of FRP tubes as a formwork, protective jacket, confinement, and shear and flexural reinforcement. The FRP tubes could also be used to complement or replace conventional steel reinforcement of the column. Concrete-filled FRP tubes were instrumented and tested under uniaxial compressive load. Results indicated that external confinement of concrete by FRP tubes can significantly enhance the strength, ductility, and energy absorption capacity of concrete.

Numerous experimental studies on small-scale concrete specimens confined with various FRP composites have been conducted in recent decades (Xiao and Wu 2003; Rahai et al. 2008; Benzaid et al. 2010; Piekarczyk et al. 2011; Wang et al. 2012; Khairallah 2013; Touhari and Mitiche-Kettab 2016; Guo et al. 2016; Chengala et al. 2018; Rahman et al. 2018). These experimental tests were designed to examine the behaviour of different-sized FRP-wrapped concrete specimens subjected to uniaxial compression up to failure. The effects of several parameters, including unconfined concrete strength, types of FRP composites, and the number of FRP layers were experimentally investigated. Test results demonstrated that various types of FRP composites expressively increased the strength and ductility of plain concrete specimens.

Analytical equations based on experimental data were proposed to calculate the strength of FRP-confined concrete with circular, square, and rectangular cross sections (Shehata et al. 2002; Ilki and Kumbasar 2003; Youssef et al. 2007 and others). The estimations given by proposed equations were compared with the experimental results. It was concluded

that estimating the compressive strength of confined concrete using proposed equations was dependent on the cross-sectional shape.

The comparative studies of numerical and experimental methods concerning concrete cylinders confined by FRP composites have been studied by Sadeghian et al. (2008), Chakrabarti et al. (2008), Elsanadedy et al. (2012), Seffo and Hamcho (2012), Delnavaz and Hamidnia (2015), and Al-Sodani et al. (2018). In the above-mentioned studies, uniaxial compression tests were carried out on cylindrical concrete specimens. Using the validated numerical model, the stress–strain behaviour of confined concrete has been examined.

The stress–strain behaviour of specimens discontinuously or partially confined with various types of FRP composites has been examined by Toutanji and Saafi (2002), Campione (2006), Park et al. (2008), Camille et al. (2009), Varma et al. (2009), Ranolia et al. (2013) and Zeng et al. (2018). The obvious conclusion to be drawn from the above-mentioned research is that the confinement effectiveness improves with an increase in the number of wraps.

Numerous numerical and experimental investigations have been conducted into the behaviour of specimens fully confined with various types of FRP composites as well as partially confined specimens. The previous research studies have been conducted separately for either partially confined concrete cylinders (e.g. Campione et al. 2015; Al Abadi et al. 2019) or discontinuously confined concrete cylinders (e.g. Barros and Ferreira 2008; Pham et al. 2015; Zeng et al. 2018). However, there has been relatively little research that draws a comparison of the confinement effectiveness between CFRP partial and discontinuous wrapping strengthening technique. In this study, distinction has been drawn between CFRP partial and discontinuous wrapping schemes. Concrete columns can be discontinuously wrapped with several longitudinally discrete CFRP laminates strips (e.g. C2, C4-4, C5-4, and C5-3 in Fig. 1), or alternatively partially wrapped with CFRP wraps applied at either columns' mid-height or opposite ends (e.g. C5-2, C10-2, C10, and C20 in Fig. 1). Therefore, it is of great significance to investigate the confinement effectiveness of columns discontinuously and partially wrapped versus columns fully wrapped with CFRP laminates. In other words, this article aims to clarify how different positions and widths of CFRP laminates affect the stress–strain behaviour of concrete specimens. A series of discontinuously and partially CFRP-confined circular specimens have been simulated using ABAQUS (2012), a finite element software package. The stress–strain behaviour of two types of CFRP-confined specimens modelled in ABAQUS (2012) was validated by the results obtained from the experimental program. In addition, the axial stress and strain of cylindrical specimens confined with different arrangements of CFRP laminates were compared with each

Fig. 1 Patterns of fibre wrapping

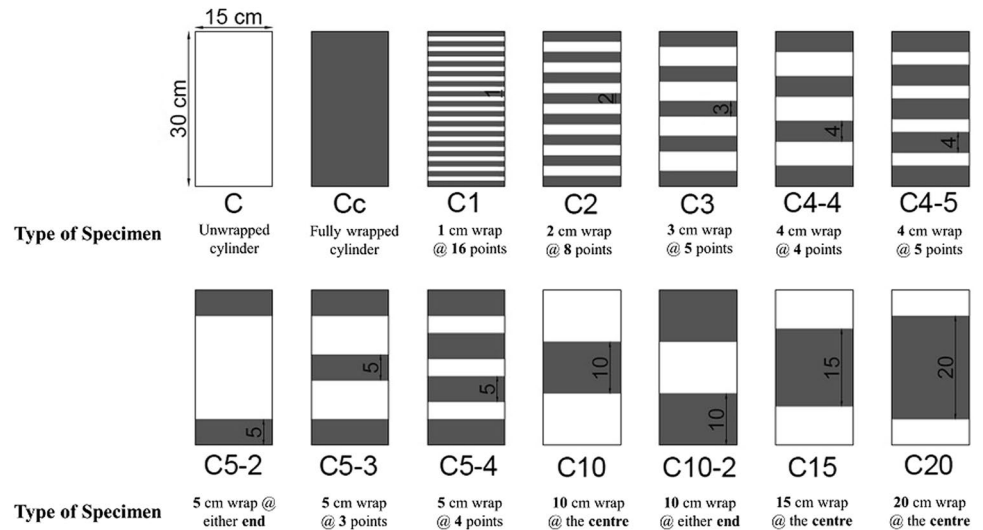


Table 1 Mix proportion of concrete

Component	Quantity (kg/m ³)
Water	195
Cement	390
Fine aggregates	935
Coarse aggregates	830

other. And finally, the typical failure mode of discontinuously CFRP-wrapped cylinders has been examined. In summary, this study has provided a context for gaining a greater understanding of the marked effect of various arrangements of CFRP laminates on the axial stress–strain of cylindrical concrete specimens.

2 Experimental Program

The experimental program was primarily designed to investigate the compressive behaviour of fully and partially CFRP-confined concrete cylinders subjected to uniaxial compression loading. A total of 12 small-scale unreinforced concrete cylinders with an outer diameter of 150 mm and a height of 300 mm were prepared with a similar mixture design. With the exception of three specimens, the other ones were partially or discontinuously wrapped with one layer of unidirectional CFRP.

2.1 Specimen Preparation

Type II Portland cement, natural sand, gravel, and water were mixed and introduced into standard cylindrical formworks to form the concrete specimens. Concrete mix design proportions are shown in Table 1. The maximum size of

the coarse aggregates was approximately 19 mm. In this study, the density of 2350 kg/m³ and w/c ratio of 0.5 for the batch of concrete were chosen to achieve the target strength of 28 MPa at 28 days. However, the actual compression strength of plain specimens on the test day was measured 36 MPa. The concrete specimens were demoulded at 24 h after casting and immersed in water for 28 days. Having been cured, the cylindrical concrete specimens were prepared for the wrapping stage.

Torayca yarn (T700 s), a high-performance carbon fibre made of polyacrylonitrile (PAN), and two-part epoxy laminating system were utilized for full and partial wrapping of the specimens. The selected epoxy was composed of two components: a resin (epoxy-based EPL 1012), and a hardener (EPH 112), with the weight mix ratio of 12%: 100 (Resin): 12 (Hardener). The low viscosity of EPL 1012 allows for complete impregnation of carbon fibre reinforcement, making it suitable for the wet lay-up processing method. The mechanical and physical properties of fibre and epoxy adhesive are shown in Tables 2 and 3, respectively, as provided by the manufacturer. No straight tensile coupon tests were carried out. The mechanical properties of CFRP composite are cited in Table 4, as provided by the material manufacturer.

Before starting the wrapping process, the thin layer of dust which covered the cylinders was completely removed using an air compressor. Afterwards, using a pair of scissors, CFRP laminates were cut into strips with desired lengths and widths. The process was developed by blending epoxy resin and hardener in the aforementioned ratio and giving the mixture a good stir to form a light grey paste. It is worth mentioning that the surface of cylinders should be thoroughly dry before applying the light coat of mixed epoxy. Being kept upright, the cylinders were completely coated with a layer of mixed epoxy using a paintbrush. The next phase

Table 2 Mechanical and physical properties of carbon fibre reinforcement (T700 s)

Properties	Value	Standard
Tensile strength (MPa)	4900	Torayca TY-030B-01 test method ^a
Tensile modulus (GPa)	230	Torayca TY-030B-01 test method
Strain at failure (%)	2.1	Torayca TY-030B-01 test method
Density (g/cm ³)	1.8	Torayca TY-030B-02 test method ^b
Filament diameter (μm)	7	–

^aMethod for determination of tensile strength, tensile modulus of elasticity, and elongation at break (Toray Carbon Fibres America, Inc.)

^bMethod for determination of density (Toray Carbon Fibres America, Inc.)

Table 3 Mechanical and physical properties of epoxy adhesive

Properties	Value	Test method
Tensile strength (MPa)	74.62	ASTM D638 M
Tensile modulus (GPa)	2.73	ASTM D638 M
Viscosity at 25 °C (mPa s)-EPL 1012	900–1100	–
Viscosity at 25 °C (mPa s)-EPH 112	30	–
Full cure at 25 °C (days)	7	–

Table 4 Mechanical properties of CFRP composite (T700 s)

Properties	Value	Standard
Tensile strength (MPa)	2860	ASTM D-3039
Tensile modulus (GPa)	134	ASTM D-3039
Strain at failure (%)	2.02	ASTM D-3039

was to carefully wrap the CFRP laminates strips or wraps around cylindrical specimens, with fibres oriented only in the hoop direction. A minimum overlap length of 75 mm between either end of strips was employed in order to provide fully developed tensile strength of CFRP laminates. The process culminated in applying the epoxy on the surface of

the installed sheets, thereby fully saturating the CFRP laminates strips. The concrete specimens treated with different wrap positions and various types of cylinders confined with CFRP laminates in the laboratory are given in Figs. 1 and 2, respectively.

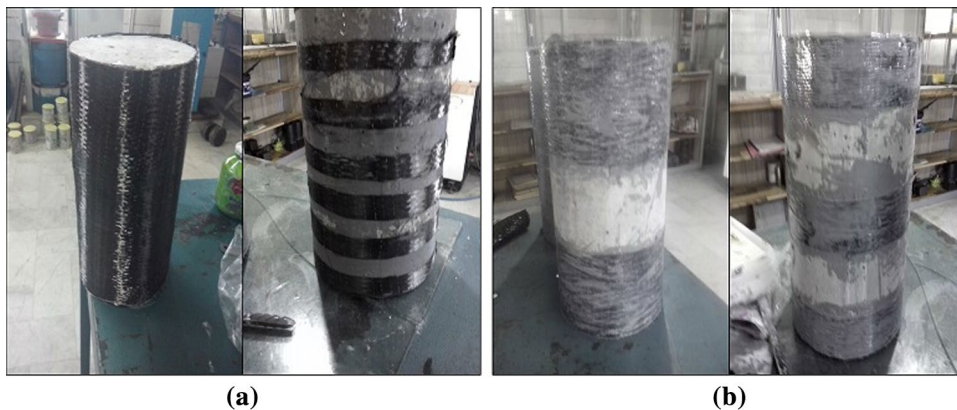
2.2 Test Setup and Loading

The wrapped specimens were exposed to the ambient temperature at least 7 days before axial loading with the aim of curing CFRP, as suggested by the material manufacturer. In order to provide uniform pressure on the top and bottom surfaces of cylinders, both ends of cylindrical specimens were capped with high-strength sulphur. All specimens were tested under monotonic concentric axial compression, using a 2000 kN load-carrying capacity hydraulic testing machine. The upper platen of the machine is fixed while the lower one moves upward according to the input displacement rate. The machine is equipped with a data acquisition system, recording the imposed load. The loading rate was 0.28 MPa/s, following the ASTM C39/C39 M-04 standard (ASTM 2003). In this study, the experimental stress–strain curves were terminated at the point when CFRP rupture occurred.

3 Numerical Modelling

A nonlinear three-dimensional finite element model of CFRP-confined concrete cylinders was developed using the finite element analysis (FEA) software ABAQUS (2012). The numerical model was validated by comparing the numerical results with the data obtained from the experimental program. The comparative study examined the numerical and experimental stress–strain behaviour of confined and unconfined concrete.

Fig. 2 Various types of cylinders confined with CFRP laminates in the laboratory: **a** before applying epoxy resin, **b** after applying the second layer of epoxy resin on the CFRP composites' layer



3.1 Material Properties

3.1.1 Concrete

Owing to the tri-axial stress state of the concrete core in partially or fully wrapped cylinders caused by both axial loading and circumferential pressure, the constitutive model should be developed in such a way that it could accurately portray the behaviour of FRP-confined concrete. The concrete damaged plasticity (CDP) material model has been employed in this study to simulate the nonlinear behaviour of confined concrete. The model is capable of considering two main failure modes of concrete, including tensile cracking and compressive crushing (ABAQUS 2012).

The model makes use of the yield function of Lubliner et al. (1989), with the modifications proposed by Lee and Fenves (1998) to account for different evolutions of strength under tension and compression (ABAQUS 2012). The evolution of the yield surface is controlled by two hardening variables, tensile and compressive equivalent plastic strains ($\bar{\epsilon}_t^{pl}$ and $\bar{\epsilon}_c^{pl}$), linked to failure mechanisms under tension and compression loading, respectively. In terms of effective stresses, the mathematic expression for F is (ABAQUS 2012):

$$F = \frac{1}{1 - \alpha} \left(\sqrt{3\bar{J}_2} - \alpha\bar{I}_1 + \beta(\bar{\epsilon}^{pl})\langle -\bar{\sigma}_{min} \rangle - \gamma\langle -\bar{\sigma}_{min} \rangle \right) - \bar{\sigma}_c(\bar{\epsilon}_c^{pl}) = 0 \tag{1}$$

with

$$\alpha = \frac{\frac{f'_b}{f'_{co}} - 1}{2\frac{f'_b}{f'_{co}} - 1}; \quad 0 \leq \alpha \leq 0.5, \tag{2}$$

$$\beta = \frac{\bar{\sigma}_c(\bar{\epsilon}_c^{pl})}{\bar{\sigma}_t(\bar{\epsilon}_t^{pl})}(1 - \alpha) - (1 + \alpha), \tag{3}$$

$$\gamma = \frac{3(1 - K_c)}{2K_c - 1} \tag{4}$$

where \bar{I}_1 is the first invariant of the effective stress, \bar{J}_2 is the second invariant of the effective stress, f'_b is the biaxial concrete strength, f'_{co} is unconfined concrete cylinder strength, σ_{min} is the minimum principal effective stress, $\bar{\epsilon}^{pl}$ is the equivalent plastic strain, $\bar{\sigma}_c$ is the effective compressive cohesion stress, $\bar{\sigma}_t$ is the effective tensile cohesion stress, K_c is the ratio of biaxial concrete strength to tri-axial compression strength, and the Macauley bracket $\langle \cdot \rangle$ is defined by $\langle x \rangle = (|x| + x)/2$ (Zeng et al. 2018a, b).

The non-associated plastic flow potential used in the CDP model is the Drucker–Prager hyperbolic function (Drucker and Prager 1952), given by Eq. (5):

$$G = \sqrt{(e\sigma_{10} \tan \psi) + \bar{J}_2} - \bar{I}_1 \tan \psi \tag{5}$$

where e is the flow potential eccentricity of the hyperbolic function, which defines the rate at which the function approaches the asymptote (the flow potential tends to a straight line as the eccentricity tends to zero), σ_{10} is the uniaxial tensile stress at failure, and ψ is the dilation angle. Due to the explicit procedure employed in this study, the viscosity parameter was automatically set to zero by the package. The predefined constants for three input parameters of the plastic part of the CDP model (f'_b/f'_{co} , e , K_c) proposed by ABAQUS (2012) Analysis User’s Manual were considered in this study. Table 5 shows the elastic and plastic parameters of the CDP model.

In addition to the above-mentioned parameters, the uniaxial tensile and compressive response of concrete were defined in the material model. The uniaxial compression hardening curve is defined in terms of the inelastic strain, ϵ_c^{in} , which is calculated using Eq. (6). The damage plasticity model automatically calculates the compressive plastic strains, ϵ_c^{pl} Eq. (7), using a damage parameter, d_c , that represents the degradation of the elastic stiffness of the material in compression.

$$\epsilon_c^{in} = \epsilon_c - \frac{\sigma_c}{E_c} \tag{6}$$

$$\epsilon_c^{pl} = \epsilon_c^{in} - \frac{d_c}{(1 - d_c)} \frac{\sigma_c}{E_c} \tag{7}$$

where σ_c and ϵ_c are the compression stress and strain of the concrete, respectively. E_c (MPa) is the modulus of elasticity of the concrete calculated using the equation proposed by American Concrete Institute Committee 318 (2008):

$$E_c = 4730\sqrt{\sigma_c} \tag{8}$$

The damage variable d_c is defined based on Eq. (9) (Yu et al. 2010):

Table 5 Elastic and plastic parameters of the CDP model

Elastic properties	
Young’s modulus (MPa)	28,380
Poisson’s ratio	0.2
Plastic properties	
Dilation angle (degree)	30°
Eccentricity	0.1
f'_b/f'_{co}	1.16
K_c	0.667

$$d_c = 1 - \frac{\sigma_c}{f'_{co}} \quad (9)$$

Kent and Park (1971) concrete model presenting both unconfined and confined concrete behaviour under compressive loading was adopted in this study. The ascending curve of this model is represented by:

$$\sigma_c = f'_{co} \left[\frac{2\varepsilon_c}{\varepsilon_{cc}} - \left(\frac{\varepsilon_c}{\varepsilon_{cc}} \right)^2 \right] \quad (10)$$

where ε_{cc} is the strain value corresponding to this maximum stress. The value of $\varepsilon_{cc} = 0.002$ is used in this study which is proposed by Park and Paulay (1975). The behaviour of concrete from the outset in Eq. (10) is considered to be non-linear. However, the stress–strain response of concrete under uniaxial compression was considered to be linear up to the initial yield stress, which is assumed to be $0.4f'_{co}$ in the current study. For the sake of simplicity, moreover, instead of being a straight line, the descending branch of Kent and Park (1971) model was assumed to be similar to the ascending one. The stress–strain relationship curve of concrete for different values of ε_c is plotted using the above equations, and this curve is shown in Fig. 3a. Figure 3b shows axial stress versus inelastic strain curve for compression hardening of concrete.

When modelling confined concrete, the tensile behaviour usually is of less importance. However, the stress–strain curve in tension was assumed to be linearly elastic until the tensile strength (10% of compressive strength), followed by a dramatic linear decrease to zero. In order to avoid numerical instability, 1% of tensile strength instead of zero was considered in the constitutive model. The corresponding cracking strain of this tensile strength was assumed to be 0.0012 (Abbassi and Dabbagh 2014).

3.1.2 CFRP Jacket

The CFRP jacket is generally assumed to have a linear elastic behaviour until rupture. Hence “Lamina” material type, which is provided by ABAQUS (2012) to model orthotropic elastic materials, has been assigned to the elastic properties of CFRP jacket. The unidirectional lamina has three mutually orthogonal planes of material properties (1, 2 and n) which are referred to as the principal material coordinates. The 1 and 2 principal directions are aligned with the direction of fibres and axial loading, respectively, while n is normal to the CFRP sheet plane (Salameh 2015). As the fibres in the CFRP jackets considered in the present study are all oriented in the hoop direction, the stiffness in the axial direction (loading direction) is negligibly small. The modulus of elasticity in the hoop direction (E_1) was defined in accordance with ASTM standard D3039 (ASTM 2008), as provided by the material manufacturer (Table 4). By contrast, the modulus of elasticity in the axial direction (E_2) and the shear modulus were both assumed to have a very small value so that the unidirectional CFRP laminate was not affected by interaction with other directions (e.g. 0.001 GPa). The Poisson’s ratio was set equal to zero, and the thickness of the CFRP laminates was assumed to be 0.165 mm in the numerical model.

3.2 Model Geometry

Three-dimensional models of fully or partially CFRP-confined concrete cylinders were established in ABAQUS (2012) in order to investigate the effect of different arrangements of CFRP laminates on the stress–strain behaviour of specimens. The three-dimensional concrete cylinder and the CFRP shell were assembled between two discrete rigid plates. Two reference points were assigned to both rigid

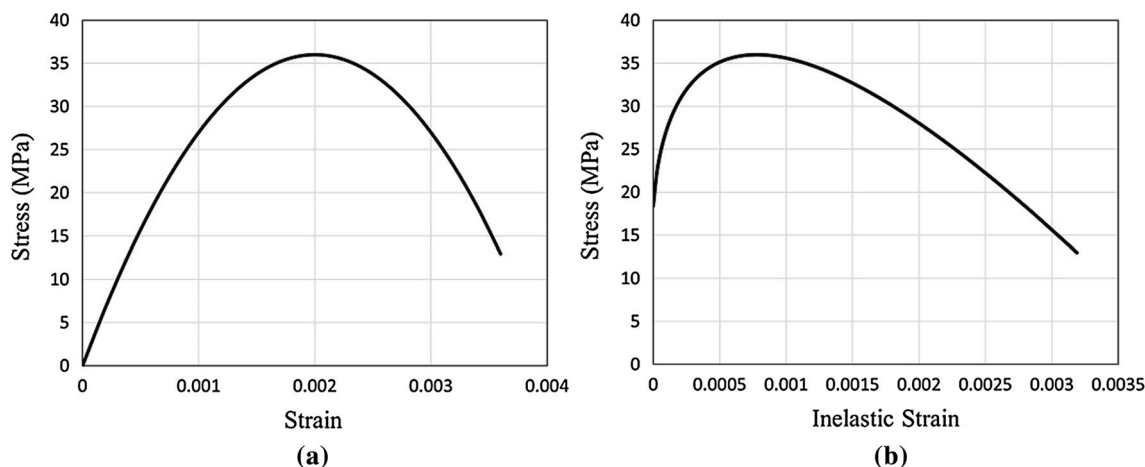


Fig. 3 Stress–strain relationship curve of concrete for compression hardening **a** stress versus total strain and **b** stress versus inelastic strain

plates with the aim of recording the amount of axial displacement and reaction force variations with time.

3.3 Boundary Conditions and Analysis Step

A dynamic explicit type of analysis in ABAQUS (2012) was employed in this study as convergence difficulties with the CDP model are fewer with explicit analysis. Furthermore, this type of analysis creates the possibility of using the displacement control regime with a defined rate of displacement imposing in the axial direction of the cylinder in the analysis. The displacement control means that the uniaxial compressive displacements instead of the compressive loads were specified as a boundary condition in the software (Labibzadeh et al. 2017). With the exception of vertical displacement of the reference point of the top rigid plate, all degrees of freedom were restrained for the reference points of top and bottom rigid plates. In all the FEA, axial displacement was imposed by the discrete rigid plate on the top surface of the concrete cylinder until the CFRP rupture strain (in the hoop direction) reached 60% of the ultimate tensile strain provided by the material manufacturer (i.e. 1.2%). This limit for CFRP rupture strain was defined based on the experimental observation reported by previous researchers (Xiao and Wu 2000; Valdmans et al. 2007; Zeng et al. 2018a, b).

3.4 Interaction

The interaction between CFRP jacket and the concrete cylinder was defined as a surface tie constraint, with the master surface being the surface of the concrete cylinder and the slave surface being the inner surface of the CFRP shell. Finer mesh was assigned to the slave surface for better convergence performance. Regarding the interaction between both top and bottom discrete rigid plates, which records the history output of displacement along the height of the

cylinder and the reaction force, respectively, and the concrete cylinder, the penalty formulation for tangential behaviour with a friction coefficient of 0.25 and the hard contact for normal behaviour was defined (Ellobody et al. 2006; Dai and Lam 2010).

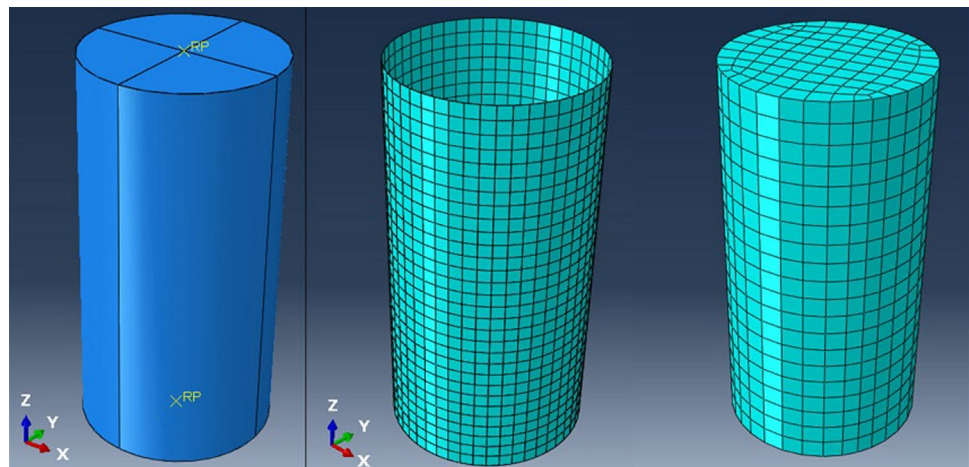
3.5 Mesh and Element Type

Both the concrete cylinder and CFRP jacket were partitioned for the purpose of uniform meshing. Concrete was modelled using an 8-node linear brick, reduced integration element (C3D8R). The CFRP jacket was modelled using a 4-node doubly curved thick shell, reduced integration element (S4R). The approximate element size of CFRP jacket was smaller, about two-thirds the element size of the concrete cylinder, which guaranteed a good adjustment at the curved contact surface. Mesh convergence studies were conducted for the numerical model to provide fairly accurate results with relatively low computational time. The approximate global mesh size of 15 mm and 10 mm was adopted for concrete and CFRP, respectively. The FE model and the mesh adopted for different parts of the model is shown in Fig. 4.

4 Model Validation

The proposed FE model was validated against the experimental results. In this study, the results of two types of specimens mentioned in Fig. 1 (C and C10) were analysed for FEM verification. In fact, the axial stress–strain behaviour of the above-mentioned specimens obtained from the laboratory measurement has been used for validation purposes. Three gauges accurate to 0.01 mm were used for strain calculation. Two of them were installed on the ring, measuring the axial and radial strain of the concrete cylinder. The last one, which was attached to the adjustable platen, measured the movement of the platen. It is worth mentioning that only

Fig. 4 Finite element mesh



the axial strain of the concrete cylinder was compared with the corresponding output in ABAQUS (2012). Hence, the measurements recorded from the other two dial gauges were used as control data.

Figure 5 illustrates the instrumentations for the concrete cylinder in the compression test. The comparison between the experimental and the FEA results for the unwrapped specimen (C) is plotted in Fig. 6. As can be seen, there is a good agreement between the stress–strain behaviour of numerical predictions and experimental results. In the case of specimen C10, moreover, a theoretical stress–strain model for concrete confined by FRP composites developed by Youssef et al. (2007) has been provided for the purpose of comparison. This proposed model was verified using both the experimental data produced from the authors' study and other reliable data from previously published data. Their comprehensive experimental program included large-scale circular, square and rectangular short columns confined by carbon/epoxy and E-glass/epoxy jackets providing a wide range of confinement ratios. This constitutive model predicts the ultimate strength, ultimate stain and depicts the entire stress–strain diagram for CFRP-confined concrete specimens. Figure 7 compares the experimental and numerical stress–strain curves with the theoretical curves generated by Youssef et al. (2007) for the specimen confined with 10-cm



Fig. 5 Instrumentations for the concrete cylinder in the compression test

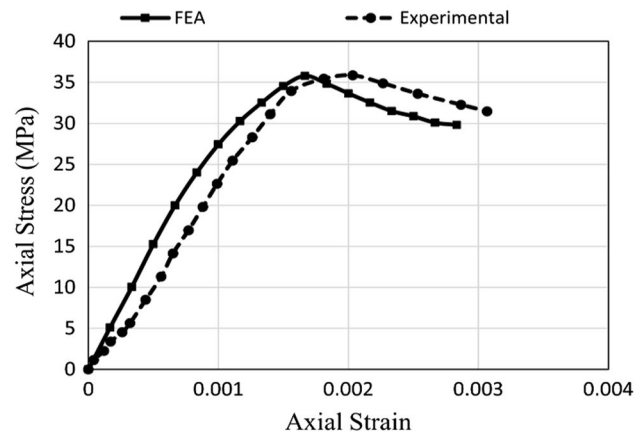


Fig. 6 Comparison between numerical and experimental results for the unwrapped specimen (C)

wrap at the centre (C10). The predicted axial stress–strain curves showed a two-segment behaviour, while both experimental and numerical axial stress–strain curves exhibit a three-segment behaviour, and the stresses within the transition section was generally underestimated by the Youssef et al. (2007) model. Vincent and Ozbakkaloglu (2015) also reported the partially FRP-confined concrete exhibits a transition segment when the FRP confinement is not completely activated.

It can be seen from Fig. 7 that the predicted axial stress is lower than the experimental axial stress when the axial strain is small. This discrepancy between experimental and predicted axial stress within the low strains was also reported by Zeng et al. (2018a, b).

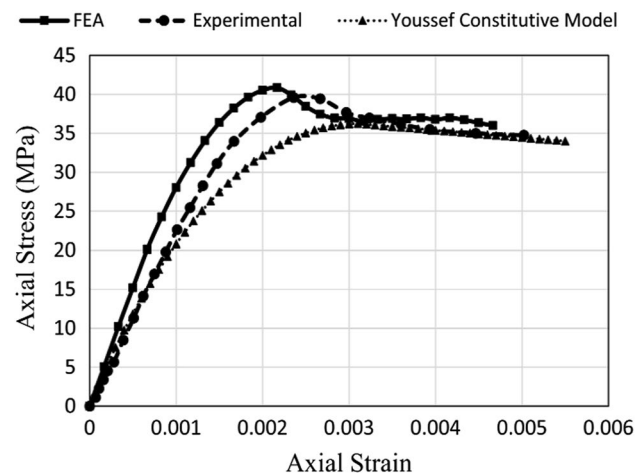


Fig. 7 Comparison between numerical, experimental, and Youssef et al. (2007) constitutive model results for the specimen wrapped with 10-cm wrap at the centre (C10)

Comparative study of experimental and FE curves in Fig. 7 revealed that the FE curve tends to overestimate the confined concrete stress. This reveals that the concrete confinement behaviour in CFRP-wrapped concrete cylinders is not fully achieved, compared to the perfect conditions considered in the numerical models, which means that CFRP jackets failed to generate the expected lateral stress. It is clear from Fig. 7 that there are slight differences between FE results and the experimental results within the linear elastic behaviour of the specimens (the maximum difference between the axial stress of FEA and experimental program within the linear section of the axial stress–strain curve is approximately 20%). This discrepancy between numerical and experimental results existed in findings reported by some researchers investigating confined concrete behaviours (e.g. Sadeghian et al. 2008; Yu et al. 2010).

The compressive strengths of different types of specimens obtained from FEA were also compared with those obtained from the experimental program. In the experimental program, all the specimens were undergone uniaxial compression test on the same day. Similarly, models of concrete specimens have been tested under simulated uniaxial compression loading in ABAQUS (2012). The comparison between the experimental results and the numerical results of different types of specimens is tabulated in Table 6. The numerical compressive strengths were found to be very close to those observed in the experiments. The mean value of the numerical-to-experimental compressive strength ratio is 1.03 with a standard deviation of 0.03. As shown in Table 6, the numerical results are perfectly consistent with the experimental results, indicating that the FE model can be employed to measure the confined compressive strength of CFRP-wrapped specimens.

5 Results and Discussion

5.1 Confinement Effectiveness of Different Types of Specimens

Table 7 summarizes the numerical results of different types of specimens shown in Fig. 1. It is evident that with the exception of C5-2, the other types of specimens experienced an increase in confinement effectiveness, ranging from 9 to 34%. In addition, except for C5-2 and C10-2, there was a 20–50% rise in the strain enhancement of other specimens. Apparently, reinforcement by CFRP jackets significantly increased the compressive strength and the axial strain. From Table 7, it is clearly observed that the closer to the centre of specimens CFRP jacket is wrapped, the higher compressive strength is achieved.

Figure 8 illustrates the ratio of compressive strength versus the ratio of CFRP-bonded area for different types of

Table 6 Numerical and experimental compressive strength of different types of specimens

Type of specimen	Compressive strength (MPa)		f_{num}/f_{exp}
	Experimental	Numerical	
C	35.85	35.79	1.00
Cc	45.25	47.75	1.06
C2	40.80	41.23	1.01
C4-4	38.60	40.26	1.04
C5-3	37.40	39.94	1.07
C10	39.60	40.87	1.03
C10-2	38.60	39.13	1.01
Mean			1.03
Standard deviation			0.03

specimens. In this figure, the compressive strength of the unwrapped cylinder was used as a unit (35.79); therefore, all compressive strength of specimens was divided by this unit. The ratios of compressive strength were sorted according to their values. The histogram begins with a value of 1 belonging to the unwrapped cylinder and ends with 1.33 which belongs to the fully wrapped cylinder. As the histogram clearly illustrates, the ratios of compressive strength of specimens confined with side wraps (C5-2, C10-2) pale in comparison with those of specimens confined with central wraps (C15, C20). The ratios of the compressive strength of other discontinuously wrapped specimens, however, range from 1.12 to 1.17, indicating that a change in the arrangements of discontinuous CFRP laminates (the width and number of wraps) has a relatively small effect on the ratio of compressive strength.

5.2 Comparative Stress–Strain Diagrams

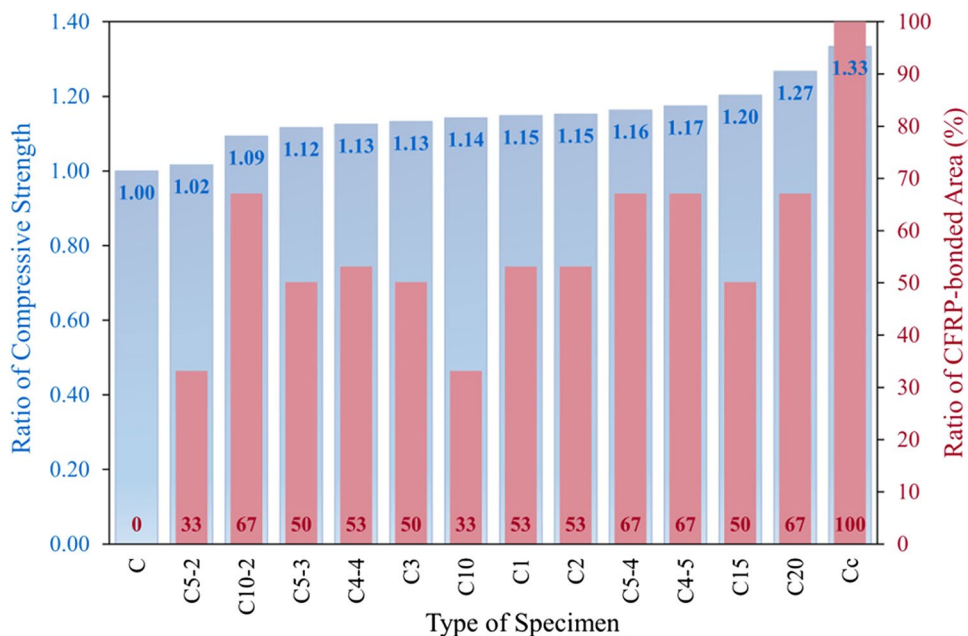
Stress–strain curves of specimens confined with the same ratio of bonding area of CFRP (CFRP-bonded area versus total area of the cylinder surface) have been compared. In all comparative studies, the stress–strain behaviour of the unwrapped and fully wrapped cylinder has been considered, providing the baseline for comparison. Figure 9 compares the axial stress–strain behaviour of unwrapped and fully wrapped specimens with ones wrapped in an equal area of CFRP jacket.

Overall, in these figures one can observe that all of the graphs begin as near-linear until the sudden failure of concrete specimens. As also observed in Fig. 9, the stress-carrying capacity and the strain capacity of the specimens wrapped with CFRP jackets improve greatly compared to the unwrapped specimen. In Fig. 9 for the discontinuously CFRP-confined concrete cylinders (C3, C5-3, C1, C2, C4-4, C4-5, and C5-4), the maximum stress recorded tends to vary approximately from 40 to 42 MPa. As was mentioned in the

Table 7 Summary of FEA results of different types of specimens

Type of specimen	Ratio of CFRP-bonded area ^a (%)	Compressive strength f_c (MPa)	Confinement effectiveness (%)	Axial strain at max strength ϵ_c	Strain enhancement (%)
C	–	35.79	–	0.00166	–
Cc	100	47.75	33.4	0.00249	50.0
C1	53	41.09	14.8	0.00216	30.1
C2	53	41.23	15.2	0.00216	30.1
C3	50	40.53	13.2	0.00200	20.5
C4-4	53	40.26	12.5	0.00200	20.5
C4-5	67	42.00	17.4	0.00200	20.5
C5-2	33	36.37	1.6	0.00183	10.2
C5-3	50	39.94	11.6	0.00200	20.5
C5-4	67	41.63	16.3	0.00216	30.1
C10	33	40.87	14.2	0.00216	30.1
C10-2	67	39.13	9.3	0.00183	10.2
C15	50	43.06	20.3	0.00233	40.4
C20	67	45.36	26.7	0.00249	50.0

^aAs a percentage of total area of the cylinder surface

Fig. 8 Ratio of compressive strength versus the ratio of CFRP-bonded area for different types of specimens

previous section, it is clear that variations in the width and number of discontinuous strips do not have marked effects on the compressive behaviour of the CFRP-reinforced cylinders; but nevertheless specimens slightly differ from one another in their ultimate axial strain. As the stress–strain curves clearly illustrate, CFRP-wrapped cylinders show a substantial increase in the deformation capacity and ductility compared to the unconfined cylinders. Ductility can be defined as the capability of materials to deform while still carry load after passing the turning point (Park et al. 2008). The specimens confined with central CFRP jacket show

more ductility than discontinuously CFRP-confined specimens. In the meanwhile, however, the unwrapped specimen and the specimens confined with side CFRP jackets show more brittle behaviour.

From Fig. 9a, the axial stress–strain behaviour of the specimen with 5-cm wrap at either end (C5-2) and the unwrapped specimen (C) follows a similar pattern. However, the compressive strength of the specimen with 10-cm wrap at the centre (C10) increases dramatically. As the lateral strain of the concrete cylinder is higher at the centre, the

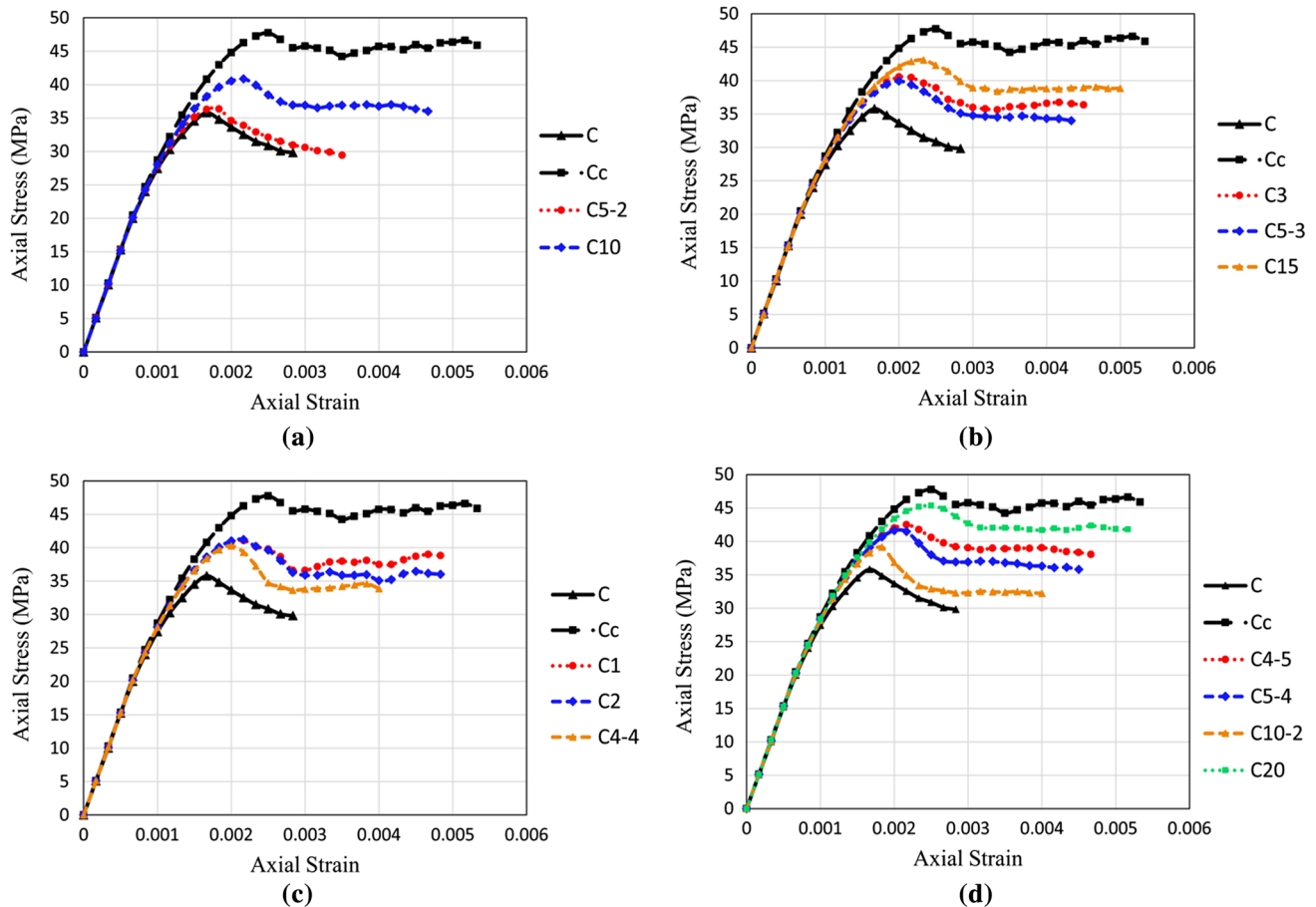


Fig. 9 Comparative axial stress–strain figures of specimens confined with an equal area of wrapped CFRP jackets

closer to the centre of specimens CFRP jacket is wrapped, the better confinement effectiveness is achieved.

Figure 9b illustrates the specimens confined with 50% ratio of CFRP-bonded area. It can be seen that the axial stress–strain behaviour of both specimens confined with 3-cm strip at 5 points (C3) and 5-cm strip at 3 points (C5-3) seems to be somewhat similar. The axial stress and strain of the specimen with 15-cm wrap at the centre (C15), by contrast, appears to be much higher.

As can be seen in Fig. 9c, both specimens confined with 1 cm strip at 18 points (C1) and 2 cm strip at 8 points (C2) are found to be similar in the axial stress–strain behaviour. Similarly, the stress–strain behaviour of both specimens confined with 4-cm strip at 5 points (C4-5) and 5-cm strip at 4 points (C5-4) are virtually equal (Fig. 9d). This means that when the specimens are interruptedly wrapped in an equal area of CFRP laminates, a change in the width and the number of strips does not have any noticeable effect on their compressive strength. In contrast, changing the position of CFRP laminates strips from the end to the centre of specimens results in the higher value of ultimate stress and strain (Fig. 8a, d).

The main conclusion to be drawn from Fig. 9 is that fully wrapping is found to be the most effective means of improving the ultimate compressive stress and strain, and thus, ductility. In many cases, nevertheless, partial or discontinuous wrapping technique looks comparatively favourable, especially for retrofitting columns not requiring considerable improvement in compressive strength as well as those which are not easily accessible (buried or immersed columns).

5.3 Failure Mode of Discontinuously CFRP-Wrapped Concrete Cylinders

When a CFRP-confined cylinder is subject to axial compression, the concrete cylinder expands laterally and this expansion is restrained by the CFRP jackets. In general, the confinement pressure provided by the CFRP jackets increases continuously with the lateral strain of concrete because of the linear elastic stress–strain behaviour of CFRP. Failure of CFRP-wrapped concrete generally occurs when the hoop rupture strength of the CFRP is reached (Teng and Lam 2004). Figure 10 shows the failure mode of discontinuously CFRP-confined concrete cylinders. The typical failure

mode for discontinuously CFRP-wrapped specimens was rupture of the CFRP shell at or near the specimen's midsection which occurred suddenly. Some crushing sounds were first heard, followed by a sudden explosive clicking sound of CFRP rupture, releasing an excessive amount of energy. CFRP jackets vertical rupture started at cylinders' mid-height and progressed upwards and downwards, triggering abrupt failure with crushing of concrete and sudden loss of load capacity. A closer examination of the midsection of the failed CFRP jackets revealed failure could be characterized by vertically continuous localized rupture. Similar observation was also reported by Vincent (2015). From Fig. 10, it can be observed that the cylinders were crushed mainly in the middle.

It should be noted that the narrow strips of CFRP laminates could be applied easily on the surface of cylinders, providing better condition for minimizing air voids. As long as the clear CFRP laminates strips spacing was small enough, the concrete between two adjacent CFRP laminates strips did not experience crushing failure. The wider the gap between two adjacent CFRP laminates strips, the larger the ineffective confinement area. The presence of a larger ineffective confinement area eventually led to localized concrete



Fig. 10 Example failure modes of discontinuously CFRP-confined concrete specimens

crushing failure, which was also reported by Zeng et al. (2018a, b). It was also observed that the concrete between adjacent CFRP laminates strips was integrated seamlessly with CFRP discontinuous jackets. The observation of the failure pattern of CFRP-confined concrete specimens can be summarized as follows. Both fully and discontinuously CFRP-confined cylinders (e.g. C1, C2, C3, C4-4, C4-5, and C5-4) show similar damage patterns.

6 Conclusions

In this study, the effect of confinement configuration of CFRP laminates strips on the axial stress–strain behaviour of concrete cylinders was numerically and experimentally investigated. Based on the results, the following conclusions can be drawn:

- The model adopted in this study to simulate the axial stress–strain behaviour of partially and fully CFRP-confined concrete cylinders revealed a good agreement with experimental results, indicating that the concrete damaged plasticity (CDP) model appeared to be capable of modelling the inelastic behaviour of CFRP-confined concrete.
- Comparison of numerical compressive strength of different types of confined specimens with experimental results (the mean value of the numerical-to-experimental compressive strength ratio was found to be 1.03 with a standard deviation of 0.03) confirmed that the FE model can be appropriate for measuring the confined compressive strength of CFRP-wrapped specimens.
- The stress-carrying capacity of partially, fully and discontinuously CFRP-wrapped specimens improved greatly compared to the plain specimen. With the exception of C5-2, CFRP laminates wrapping led to a 9–34% increase in confinement effectiveness.
- The ratios of compressive strength (maximum axial stress of confined specimen/unconfined specimen) of specimens confined with side wraps (C5-2, C10-2) pale in comparison with those of specimens confined with central wraps (C15, C20). This means that the confinement effectiveness of central CFRP wraps is much higher than that of side CFRP wraps.
- The ratios of compressive strength of discontinuously wrapped specimens range from 1.12 to 1.17, indicating that a change in the configuration of CFRP wraps (the width and number of wraps) has a relatively small effect on confinement effectiveness.
- With the exception of the fully wrapped specimen, the specimens confined with central CFRP jackets show more ductility than the discontinuously CFRP-confined specimens. In the meanwhile, however, both unwrapped

specimens and specimens confined with side CFRP jackets show more brittle behaviour.

- The wider the CFRP wrap at the centre of the specimen, the higher the strength and ductility of the CFRP-confined concrete cylinder is achieved.
- Detailed observations carried out on the typical failure pattern of discontinuously CFRP-wrapped concrete cylinders suggest that the concrete between adjacent CFRP strips is integrated seamlessly with CFRP discontinuous jackets. Hence, both fully and discontinuously CFRP-confined cylinders with a relatively small gap between CFRP laminates strips show similar damage patterns.

References

- ABAQUS (2012) ABAQUS user's and theory manuals. Dassault Systèmes Simulia Corp, Providence, RI
- Abbassi M, Dabbagh H (2014) Behavior of FRP-confined reactive powder concrete columns under eccentric loading. *J Rehabil Civil Eng* 2(1):46–64
- Al Abadi H, Paton-Cole V, Patel VI, Thai HT (2019) Axial strength and elastic stiffness behaviour of partially confined concrete columns. *Constr Build Mater* 196:727–741
- Al-Sodani AKA, Rahman MK, Al-Osta MA, Al-Gadhib AAH (2018) Finite element modeling of CFRP-strengthened low-strength concrete short columns. In: Taha M (ed) International congress on polymers in concrete (ICPIC 2018). Springer, Cham
- American Concrete Institute Committee 318 (2008) Building code requirements for structural concrete. American Concrete Institute, Detroit, MI
- ASTM (2003) Standard test method for compressive strength of cylindrical concrete specimens (C39/C39M-04). ASTM International, West Conshohocken, PA, USA
- ASTM (2008) Standard test method for tensile properties of polymer matrix composite materials (D3039M). ASTM International, West Conshohocken, PA, USA
- Barros JA, Ferreira DR (2008) Assessing the efficiency of CFRP discrete confinement systems for concrete cylinders. *J Compos Constr* 12(2):134–148
- Benzaid R, Mesbah H, Chikh NE (2010) FRP-confined concrete cylinders: axial compression experiments and strength model. *J Reinf Plast Compos* 29(16):2469–2488
- Busel J, White D (2003) CFRP and GFRP composite application for infrastructure rehabilitation and repairs. In: NASTO conference, Saratoga Spring, New York
- Camille AI, Chami P, Saad G (2009) Compressive strength of concrete cylinders with variable widths CFRP wraps: experimental study and numerical modeling. *Constr Build Mater* 23(6):2306–2318
- Campione G (2006) Influence of FRP wrapping techniques on the compressive behavior of concrete prisms. *Cement Concr Compos* 28:497–505
- Campione G, Mendola LL, Monaco A, Valenza A, Fiore V (2015) Behavior in compression of concrete cylinders externally wrapped with basalt fibers. *Compos B Eng* 69:576–586
- Chakrabarti A, Chandra A, Bharagava P (2008) Finite element analysis of concrete columns confined with FRP sheets. *J Reinf Plast Compos* 27(12):1349–1373
- Chengala RY, Vigneshkumar D, Soundara B (2018) External Strengthening of reinforced concrete column with CFRP. *Int Res J Eng Technol (IRJET)* 5(4):437–441
- Dai X, Lam D (2010) Numerical modelling of the axial compressive behaviour of short concrete-filled elliptical steel columns. *J Constr Steel Res* 66(7):931–942
- Das DC, Nizam MdEH (2014) Applications of fiber reinforced polymer composites (FRP) in civil engineering. *Int J Adv Struct Geotech Eng* 3(3):299–309
- Delnavaz A, Hamidnia M (2015) Behavior comparison of uniaxial cylindrical columns strengthened with CFRP. *J Rehabil Civil Eng* 3(2):80–88
- Drucker DC, Prager W (1952) Soil mechanics and plastic analysis for limit design. *Q Appl Math* 10(2):157–165
- Ellobody E, Young B, Lam D (2006) Behaviour of normal and high-strength concrete-filled compact steel tube circular stub columns. *J Constr Steel Res* 62(7):706–715
- Elsanadedy HM, Al-Salloum YA, Alsayed SH, Iqbal RA (2012) Experimental and numerical investigation of size effects in FRP-wrapped concrete columns. *Constr Build Mater* 29:56–72
- Guo Y, Xie J, Xie Z, Zhong J (2016) Experimental study on compressive behavior of damaged normal- and high-strength concrete confined with CFRP laminates. *Constr Build Mater* 107:411–425
- Ilki A, Kumbasar N (2003) Compressive behaviour of carbon fibre composite jacketed concrete with circular and non-circular cross-sections. *J Earthq Eng* 7(3):381–406
- Kent DC, Park R (1971) Flexural members with confined concrete. *J Struct Div* 97(7):1969–1990
- Khairallah F (2013) Mechanical behavior of confined self-compacting reinforced concrete circular columns under concentric axial loading. *Ain Shams Eng J* 4(4):461–469
- Labibzadeh M, Zakeri M, Shoaib AA (2017) A new method for CDP input parameter identification of the ABAQUS software guaranteeing uniqueness and precision. *Int J Struct Integr* 8(2):264–284
- Lee J, Fenves GL (1998) Plastic-damage model for cyclic loading of concrete. *Struct J Eng Mech* 124:892–900
- Lubliner J, Oliver S, Oller S, Onate E (1989) A plastic-damage model for concrete. *Int J Solids Struct* 25:299–329
- Park R, Paulay T (1975) Reinforced concrete structures. Wiley, New York
- Park TW, Na UJ, Chung L, Feng MQ (2008) Compressive behavior of concrete cylinders confined by narrow strips of CFRP with spacing. *Compos B Eng* 39(7):1093–1103
- Pham TM, Hadi MNS, Youssef J (2015) Optimized FRP wrapping schemes for circular concrete columns under axial compression. *J Compos Constr* 19(6):1–10
- Piekarczyk J, Piekarczyk W, Blazewicz S (2011) Compression strength of concrete cylinders reinforced with carbon fiber laminate. *Constr Build Mater* 25(5):2365–2369
- Rahai AR, Sadeghian P, Ehsani MR (2008) Experimental behavior of concrete cylinders confined with CFRP composites. In: Proceedings of The 14th world conference on earthquake engineering (14 WCEE), Beijing, China
- Rahman A, Mallick M, Ghosh S (2018) Experimental behavior of FRP confined concrete cylinder wrapped by two different FRPs. *J Mater Sci Res* 7(2):18–25
- Ranolia KV, Thakkar BK, Rathod JD (2013) Effect of different patterns and cracking in FRP wrapping on compressive strength of confined concrete. *Proc Eng* 51:169–175
- Saadatmand H (2003) Study of FRP effect on concrete confinement with the aim of consolidating reinforced concrete column beams. M.Sc. thesis, Department of Civil Engineering, Yazd University, Yazd
- Saafi M, Toutanji H, Li Z (1999) Behavior of concrete columns confined with fiber reinforced polymer tubes. *Mater J* 96(4):500–509
- Sadeghian P, Rahai AR, Ehsani MR (2008) Numerical modeling of concrete cylinders confined with CFRP composites. *J Reinf Plast Compos* 27(12):1309–1321

- Salameh N (2015) Experimental and theoretical investigation on compressive behaviour of CFRP- and SFRP-confined concrete cylinders. M.Sc. thesis, Department of Civil Engineering, University of Calgary, Calgary, Alberta
- Seffo M, Hamcho M (2012) Strength of concrete cylinder confined by composite materials (CFRP). *Energy Procedia* 19:276–285
- Shehata IAEM, Carneiro LAV, Shehata LCD (2002) Strength of short concrete columns confined with CFRP sheets. *Mater Struct* 35(1):50–58
- Teng JG, Lam L (2004) Behavior and modeling of fiber reinforced polymer-confined concrete. *J Struct Eng* 130(11):1713–1723
- Touhari M, Mitiche-Kettab R (2016) Behaviour of FRP confined concrete cylinders: experimental investigation and strength model. *Period Polytech Civil Eng* 60(4):647–660
- Toutanji H, Saafi M (2002) Stress-strain behavior of concrete columns confined with hybrid composite materials. *Mater Struct* 35(6):338–347
- Valdmanis V, Lorenzis LD, Rousakis T, Tepfers R (2007) Behaviour and capacity of CFRP-confined concrete cylinders subjected to monotonic and cyclic axial compressive load. *Struct Concr* 8(3):1–14
- Varma RK, Barros JAO, Sena-Cruz JM (2009) Numerical model for CFRP confined concrete elements subject to monotonic and cyclic loadings. *Compos B Eng* 40:766–775
- Vincent TJ (2015) Axial compressive behaviour of FRP-confined high-strength concrete. Ph.D. thesis, School of Civil, Environmental and Mining Engineering, University of Adelaide, Adelaide, South Australia
- Vincent T, Ozbakkaloglu T (2015) Influence of shrinkage on compressive behavior of concrete-filled FRP tubes: an experimental study on interface gap effect. *Constr Build Mater* 75:144–156
- Wang Z, Wang D, Smith ST, Lu D (2012) CFRP-confined square RC columns. I: Experimental investigation. *J Compos Constr* 16(2):150–160
- Xiao Y, Wu H (2000) Compressive behavior of concrete confined by carbon fiber composite jackets. *J Mater Civ Eng* 12(2):139–146
- Xiao Y, Wu H (2003) Compressive behavior of concrete confined by various types of FRP composite jackets. *J Reinf Plast Compos* 22(13):1187–1201
- Youssef MN, Feng MQ, Mosallam AS (2007) Stress-strain model for concrete confined by FRP composites. *Compos B Eng* 38(6):614–628
- Yu T, Teng JG, Wong YL, Dong SL (2010) Finite element modeling of confined concrete-II: plastic-damage model. *Eng Struct* 32(3):680–691
- Zaki MK (2011) Investigation of FRP strengthened circular columns under biaxial bending. *Eng Struct* 33(5):1666–1679
- Zeng JJ, Guo YC, Gao WY, Chen WP, Li LJ (2018a) Stress-strain behavior of concrete in circular concrete columns partially wrapped with FRP strips. *Compos Struct* 200:810–828
- Zeng JJ, Guo YC, Li LJ, Chen WP (2018b) Behavior and three-dimensional finite element modeling of circular concrete columns partially wrapped with FRP strips. *Polymers* 10(3):253–282